Multicomponent Nanoparticles via Self-Assembly with Cross-Linked Block Copolymer Surfactants

Byeong-Su Kim and T. Andrew Taton*

Department of Chemistry, University of Minnesota, 207 Pleasant Street SE, Minneapolis, Minnesota 55455

We describe a simple and versatile protocol to prepare water-soluble multifunctional nanostructures by encapsulation of different nanoparticles in shell cross-linked, block copolymer micelles. This method permits simultaneous incorporation of different nanoparticle properties within a nanoscale micellar container. We have demonstrated the co-encapsulation of magnetic (γ-Fe$_2$O$_3$ and Fe$_3$O$_4$), semiconductor (CdSe/ZnS), and metal (Au) nanoparticles in different combinations to form multicomponent micelles that retain the precursor particles' distinct properties. Because these multifunctional hybrid nanostructures spontaneously assemble from solution by simultaneous desolvation of nanoparticles and amphiphilic block copolymer components, we anticipate that this can be used as a general protocol for preparing multifunctional nanostructures without explicit multimaterial synthesis or surface functionalization of nanoparticles.

Introduction

Nanoparticles exhibit novel electrical, optical, magnetic, and chemical properties that depend on their size and composition. Advances in methods for synthesizing monodisperse, single-component inorganic nanoparticles, mostly carried out in organic solvents, have enabled precise control over the composition, size, shape, and surface properties of these nanoparticles. The controlled synthesis of multicomponent nanoparticles—in which different materials are responsible for different component properties—has been more challenging. Nevertheless, there has been a number of reports describing the preparation of complex, multimaterial nanoparticles including core−shell nanoparticles,[1−4] fused particle heterodimers,[5−8] segmented nanowires,[9−11] particles coated with other particles,[12] and more sophisticated anisotropic structures.[13,14] An alternative approach used to fabricate contiguous nanoparticles from multiple materials is to incorporate different nanoparticle types into single containers, such as silica capsules,[15,16] polymer capsules,[17] or emulsion droplets.[18]

In this paper, we outline a method for fabricating multicomponent nanostructures in which different particles are simultaneously incorporated into the glassy cores of block copolymer micelles during copolymer assembly. Amphiphilic block copolymers aggregate to form micelles with predictable sizes and morphologies in solvents that are selective for one of the two copolymer blocks.[19,20] Eisenberg and co-workers have shown that these micelles are particularly stable if the core-forming block is a glassy polymer such as polystyrene,[21] and Wooley and co-workers have demonstrated that kinetic disassembly of polystyrene-core micelles can be prevented altogether by chemically cross-linking the hydrophilic shell.[22] We have previously constructed permanent hybrid nanostructures by assembling these cross-linkable polymeric surfactants around gold,[23,24] magnetic[25] and semiconductor nanoparticles,[26] as well as carbon nanotubes.[27] In this method, nanoparticles and amphiphilic block copolymers are initially mixed in a solvent that is good for all components, and then the polarity of the solvent is gradually increased to induce simultaneous desolvation of both the hydrophobic nanoparticles and the hydrophobic block of the amphiphilic copolymer. Consistent with the idea that this micelle encapsulation approach is based solely on noncovalent interactions between nanoparticles and copolymer micelle blocks, we report that it can be easily used with combinations of nanoparticles to construct multifunctional capsules possessing several desirable properties in a single-nanoscale object (Scheme 1). Herein, we describe the spontaneous assembly of combina-

* Author to whom correspondence should be addressed. E-mail: taton@chem.umn.edu.

(1) Peng, X. G.; Schlamp, M. C.; Kadavanich, A. V.; Alivisatos, A. P. *J. Am. Chem. Soc.* **1997,** *119,* 7019−7029.

(2) Teng, X. W.; Black, D.; Watkins, N. J.; Gao, Y. L.; Yang, H. *Nano Lett.* **2003,** *3,* 261−264.

(3) Zeng, H.; Li, J.; Wang, Z. L.; Liu, J. P.; Sun, S. H. *Nano Lett.* **2004,** *4,* 187−190.

(4) Kim, H.; Achermann, M.; Balet, L. P.; Hollingsworth, J. A.; Klimov, V. I. *J. Am. Chem. Soc.* **2005,** *127,* 544−546.

(5) Gu, H. W.; Zheng, R. K.; Zhang, X. X.; Xu, B. *J. Am. Chem. Soc.* **2004,** *126,* 5664−5665.

(6) Gu, H. W.; Yang, Z. M.; Gao, J. H.; Chang, C. K.; Xu, B. *J. Am. Chem. Soc.* **2005,** *127,* 34−35.

(7) Yu, H.; Chen, M.; Rice, P. M.; Wang, S. X.; White, R. L.; Sun, S. H. *Nano Lett.* **2005,** *5,* 379−382.

(8) Kwon, K. W.; Shim, M. *J. Am. Chem. Soc.* **2005,** *127,* 10269−10275.

(9) Wu, Y.; Fan, R.; Yang, P. *Nano Lett.* **2002,** *2,* 83−86.

(10) Nicewarner-Pena, S. R.; Griffith Freeman, R.; Reiss, B. D.; He, L.; Pena, D. J.; Walton, I. D.; Cromer, R.; Keating, C. D.; Natan, M. J. *Science* **2001,** *294,* 137−141.

(11) Park, S.; Lim, J. H.; Chung, S. W.; Mirkin, C. A. *Science* **2004,** *303,* 348−351.

(12) Wang, D.; He, J.; Rosenzweig, N.; Rosenzweig, Z. *Nano Lett.* **2004,** *4,* 409−413.

(13) Mokari, T.; Rothenberg, E.; Popov, I.; Costi, R.; Banin, U. *Science* **2004,** *304,* 1787−1790.

(14) Kudera, S.; Carbone, L.; Casula, M. F.; Cingolani, R.; Falqui, A.; Snoeck, E.; Parak, W. J.; Manna, L. *Nano Lett.* **2005,** *5,* 445−449.

(15) Kim, J.; Lee, J. E.; Lee, J.; Yu, J. H.; Kim, B. C.; An, K.; Hwang, Y.; Shin, C. H.; Park, J. G.; Kim, J.; Hyeon, T. *J. Am. Chem. Soc.* **2006,** *128,* 688−689.

(16) Yi, D. K.; Selvan, S. T.; Lee, S. S.; Papaefthymiou, G. C.; Kundaliya, D.; Ying, J. Y. *J. Am. Chem. Soc.* **2005,** *127,* 4990−4991.

(17) Gaponik, N.; Radtchenko, I. L.; Sukhorukov, G. B.; Rogach, A. L. *Langmuir* **2004,** *20,* 1449−1452.

(18) Mandal, S. K.; Lequeux, N.; Rotenberg, B.; Tramier, M.; Fattaccioli, J.; Bibette, J.; Dubertret, B. *Langmuir* **2005,** *21,* 4175−4179.

(19) Hamley, I. W. *Block Copolymers in Solution: Fundamentals and Applications*; John Wiley and Sons: Chichester, UK, 2005.

(20) Jonsson, B. *Surfactants and Polymers in Aqueous Solution*; Wiley: New York, 1999.

(21) Zhang, L. F.; Eisenberg, A. *Polym. Adv. Technol.* **1998,** *9,* 677−699.

(22) Huang, H. Y.; Kowalewski, T.; Remsen, E. E.; Gertzmann, R.; Wooley, K. L. *J. Am. Chem. Soc.* **1997,** *119,* 11653−11659.

(23) Kang, Y.; Taton, T. A. *Angew. Chem., Int. Ed.* **2005,** *44,* 409−412.

(24) Kang, Y.; Taton, T. A. *Macromolecules* **2005,** *38,* 6115−6121.

(25) Kim, B.-S.; Qiu, J.-M.; Wang, J.-P.; Taton, T. A. *Nano Lett.* **2005,** *5,* 1987−1991.

(26) Shibasaki, Y.; Kim, B.-S.; Young, A. J.; McCloon, A.; Ekker, S. C.; Taton, T. A., unpublished.

(27) Kang, Y.; Taton, T. A. *J. Am. Chem. Soc.* **2003,** *125,* 5650−5651.

Scheme 1.　Preparation of Multifunctional Hybrid Nanostructures by Co-encapsulation of Multiple Types of Nanoparticles (A and B) within a Cross-Linkable Block Copolymer Micelle
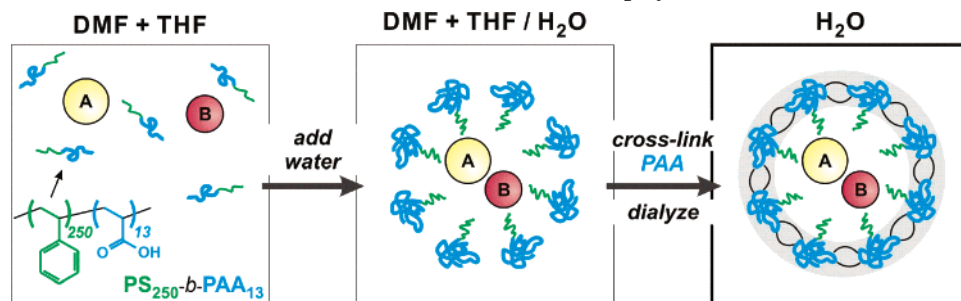
tions of magnetic (γ-Fe$_2$O$_3$ and Fe$_3$O$_4$), semiconductor (CdSe/ZnS), and metal (Au) nanoparticles within the cores of polystyrene-*block*-poly(acrylic acid) (PS-*b*-PAA) micelles.

Because each component can be prepared in monodisperse form prior to encapsulation, and because the sizes and compositions of the products can be closely controlled, the general self-assembly method introduced here provides multiple-core nanoparticles with predictable physical properties. Moreover, the product nanostructures are stable in water and aqueous buffers, which is crucial to their potential application in biology and biotechnology.

Experimental Procedures

Materials. Amphiphilic block copolymer, polystyrene$_{250}$-*block*-poly(acrylic acid)$_{13}$ (PS$_{250}$-*b*-PAA$_{13}$) was synthesized via sequential atomic transfer radical polymerization (ATRP) as previously reported.[23] Hydrophobic monodisperse magnetic γ-Fe$_2$O$_3$ ($d = 10.4$ nm) and Fe$_3$O$_4$ ($d = 4.5$ nm) nanoparticles were prepared by thermal decomposition of Fe(CO)$_5$ and Fe(acac)$_3$, respectively, as described in the literature.[28,29] Hydrophilic tetramethylammonium hydroxide (TMAOH)-stabilized magnetic γ-Fe$_2$O$_3$ nanoparticles ($d = 11$ nm) were prepared by coprecipitation of FeCl$_2$/FeCl$_3$ with reductant, following a literature protocol.[30] All core−shell type trioctylphosphine oxide (TOPO)-coated CdSe/ZnS quantum dots (QDs, $d = 2.9$ and 6.1 nm) were purchased from Evident Technologies. Two different batches of 6.1 nm CdSe/ZnS quantum dots were purchased with slight deviations in emission maximum, 626 and 618 nm, respectively. Concentrations of quantum dots were calculated by measuring the absorbance with UV−vis spectroscopy using a known molar extinction coefficient at the first exciton peak.[31] Hydrophobic oleylamine-coated Au nanoparticles ($d = 13$ nm) were prepared following a method modified from the literature.[7] *N,N*-Dimethylformamide (DMF) and tetrahydrofuran (THF) were purchased from Aldrich and used as received.

Characterization. Steady-state fluorescence spectra were taken on a Quantamaster Fluorimeter (PTI) at room temperature using an excitation wavelength (λ_{ex}) of either 365 or 400 nm and the emission wavelength (λ_{em}) set to $\lambda_{em,max}$ of QDs, with emission and excitation slit widths of 2 μm (equivalent to $\lambda = \pm2$ nm spectral width). Quantum yields (QY) were determined by the comparison of spectrally integrated emission of QD containing micelles in water with the emission of Rhodamine 6G dissolved to identical optical density (<0.015) at the same excitation wavelength ($\lambda_{ex} = 400$ nm).[32] QY measurements were performed on QD containing micelles without centrifugal purification to account for all material. Fluorescence microscopy was performed with a confocal microarray scanner

(ScanArray, Packard Bioscience). Transmission electron microscopy (TEM) images were obtained on a JEOL 1210 electron microscope equipped with a Gatan video camera and a Gatan Multiscan CCD camera (1024 × 1024 pixels). Micelle solutions were dropped onto Formvar graphite-coated copper grids (300 mesh, Electron Microscopy Science) and air-dried for TEM imaging. All images were obtained at an operating voltage of 120 kV.

Representative Co-encapsulation of Magnetic γ-Fe$_2$O$_3$ Nanoparticles and CdSe/ZnS Quantum Dots: [γ-Fe$_2$O$_3$-CdSe/ZnS]@PS-*b*-PAA$_{XL}$. First, appropriate volumes of 10.4 nm oleic acid-stabilized γ-Fe$_2$O$_3$ magnetic nanoparticles (1.0 mg/mL in THF) and 6.1 nm TOPO-stabilized CdSe/ZnS nanoparticles (0.1 mg/mL in THF) were mixed in a ratio calculated to give the desired number of particles in the final nanostructures. A freshly prepared 100 μL PS$_{250}$-*b*-PAA$_{13}$ solution (1.0 mg/mL in DMF) was then added slowly, with vigorous stirring, to the nanoparticle mixture such that [γ-Fe$_2$O$_3$]$_{initial}$ = 0.10 mg/mL, [CdSe/ZnS]$_{initial}$ = 2.0 × 10^{-3} mg/mL, and [PS$_{250}$-*b*-PAA$_{13}$]$_{initial}$ = 0.10 mg/mL in 20:80 (v/v) DMF/THF (total volume of solution 1.0 mL). Then, 4.0 mL of Millipore water (18 MΩ cm) was gradually added to the solution at a rate of 140 mL/h with vigorous stirring. After stirring for 30 min, the resulting suspension was subjected to dialysis against Millipore water for over 24 h (Spectra/Por 4 Regenerated Cellulose Membrane, MWCO = 12 000−14 000) to remove any residual solvent. Further cross-linking of 50% of the carboxylic acids in the acrylate shell of the micelle was carried out as described previously.[25] The cross-linked micelle suspensions were subjected to centrifugation at low speed (2940*g* RCF$_{avg}$, 25 min). The bottom 10% of the solution was discarded to remove any macroscopic aggregates; TEM analysis showed these to be large aggregates of polymer micelles with both magnetic and quantum dot nanoparticles. The main purpose of this centrifugation at low speed was to remove these heavily loaded aggregates and to narrow the particle distribution in the micelle core. Another round of centrifugation was performed on the recovered supernatant (85 000*g* RCF$_{avg}$, 25 min) to isolate product micelles. The upper 90% of this solution, which did not appear fluorescent under a UV lamp, was discarded, and the same volume of Millipore water was added to the solution. This procedure was repeated twice to ensure purification. The resulting [γ-Fe$_2$O$_3$-CdSe/ZnS]@PS-*b*-PAA$_{XL}$ micelles were readily redispersed in water. After the purification steps, 2.0 μL of the resulting solution was deposited on the TEM grid and dried in air before taking TEM images.

To prepare [γ-Fe$_2$O$_3$-CdSe/ZnS]@PS-*b*-PAA$_{XL}$ in pure THF, the procedure described previously was followed except that THF was used as the initial organic solvent (instead of the DMF/THF mixture) and the rate of water addition was increased to 400 mL/h.

Results and Discussion

As illustrated in Scheme 1, our primary goal was to prepare multicomponent nanostructures in which different nanoparticles were incorporated in micelle containers. In principle, these composite micelles should incorporate different properties in the same nanostructures. To test the overall concept, we first co-encapsulated magnetic γ-Fe$_2$O$_3$ nanoparticles ($d = 10.4$ nm)

(28) Hyeon, T.; Lee, S. S.; Park, J.; Chung, Y.; Na, H. B. *J. Am. Chem. Soc.* **2001**, *123*, 12798−12801.

(29) Sun, S. H.; Zeng, H.; Robinson, D. B.; Raoux, S.; Rice, P. M.; Wang, S. X.; Li, G. X. *J. Am. Chem. Soc.* **2004**, *126*, 273−279.

(30) Lyon, J. L.; Fleming, D. A.; Stone, M. B.; Schiffer, P.; Williams, M. E. *Nano Lett.* **2004**, *4*, 719−723.

(31) Yu, W. W.; Qu, L.; Guo, W.; Peng, X. *Chem. Mater.* **2003**, *15*, 2854−2860.

(32) Donega, C. D.; Hickey, S. G.; Wuister, S. F.; Vanmaekelbergh, D.; Meijerink, A. *J. Phys. Chem. B* **2003**, *107*, 489−496.
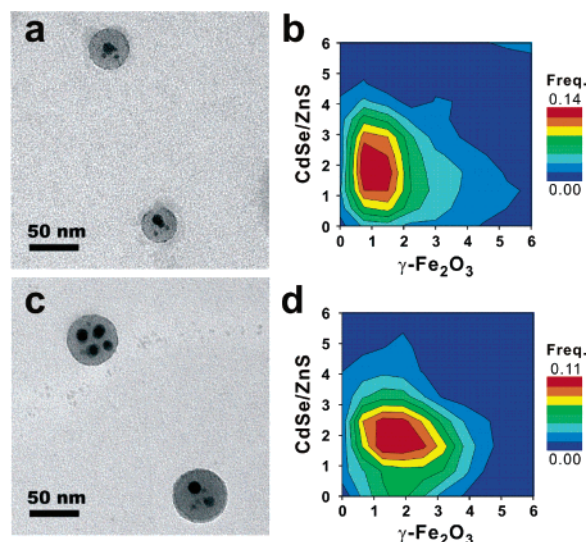
Figure 1. (a and c) TEM micrographs of cross-linked [γ-Fe$_2$O$_3$-CdSe/ZnS]@PS-*b*-PAA micelles containing both larger ($d = 10.4$ nm) magnetic γ-Fe$_2$O$_3$ and smaller ($d = 6.1$ nm) CdSe/ZnS quantum dot nanoparticles. (b and d) Distribution of particle populations found in each micelle, as counted from TEM micrographs. Initial particle concentrations for each preparation were (a and b) [γ-Fe$_2$O$_3$]$_{initial}$ = 0.10 mg/mL and [CdSe/ZnS]$_{initial}$ = 2.0×10^{-3} mg/mL (a number ratio of γ-Fe$_2$O$_3$ to CdSe/ZnS = 5) and (c and d) [γ-Fe$_2$O$_3$]$_{initial}$ = 0.20 mg/mL and [CdSe/ZnS]$_{initial}$ = 2.0×10^{-3} mg/mL (a number ratio of γ-Fe$_2$O$_3$ to CdSe/ZnS = 10). Precursor particles were dissolved in a mixture of 1.0 mL of DMF/THF (20 vol % DMF). Note that the centrifugation process removes large aggregates and also alters the ratio of the two particle types in the remaining product relative to starting material.

Figure 2. Dual properties of magnetic and fluorescent nanoparticle encapsulated micelles. (a) Suspensions of [γ-Fe$_2$O$_3$-CdSe/ZnS]@PS-*b*-PAA$_{XL}$ micelles in the absence (left) and presence (right) of a bar magnet. Suspensions were illuminated under a UV lamp (λ_{ex} = 365 nm). (b) Fluorescence micrograph of [γ-Fe$_2$O$_3$−CdSe/ZnS]@PS-*b*-PAA$_{XL}$ micelles dried on a glass slide under external magnetic field (NdFeB magnet, $H_{estimated}$ = 0.3 T at 0.5 cm). Note that the line is not formed from the solvent drying boundary. (c) Relative fluorescence emission spectra of QDs, before and after encapsulation with γ-Fe$_2$O$_3$ in PS-*b*-PAA$_{XL}$ micelle, normalized to relative quantum yield.

and fluorescent CdSe/ZnS nanoparticles ($d = 6.1$ nm)[33] within polystyrene$_{250}$-*block*-poly(acrylic acid)$_{13}$ (PS$_{250}$-*b*-PAA$_{13}$) to afford magnetic and fluorescent [γ-Fe$_2$O$_3$-CdSe/ZnS]@PS-*b*-PAA$_{XL}$ micelles. The synthetic route toward [γ-Fe$_2$O$_3$-CdSe/ZnS]@PS-*b*-PAA$_{XL}$ is easy and straightforward. Separately prepared hydrophobic magnetic γ-Fe$_2$O$_3$ nanoparticles and CdSe/ZnS quantum dots were combined with a solution of PS$_{250}$-*b*-PAA$_{13}$ in either pure THF or a DMF/THF solvent mixture. While stirring vigorously, water was gradually added to this mixture to simultaneously encapsulate both the magnetic and the quantum dot nanoparticles within the hydrophobic core of an assembled micelle. The resulting suspension was dialyzed, and the hydrophilic PAA block of the micelle was permanently cross-linked (50% of acrylate group) with a hydrophilic diamine using EDC chemistry.[23,27,34] The resulting micelle suspension was further purified by successive cycles of centrifugation, affording the magnetic and quantum dot nanoparticles simultaneously confined within a micelle core (Figure 1).

In general, the characteristics of the assembled micelles—including size, number, and type of encapsulated particles and physical properties—were determined entirely by the starting materials. TEM images (Figure 1a,c) demonstrate that both γ-Fe$_2$O$_3$ and CdSe/ZnS particles were exclusively confined within the hydrophobic cores of the micelles. The sizes of the objects depended on the number of encapsulated particles but were typically 40−50 nm in diameter. Both particle types were clearly discerned by differences in their size and contrast in the TEM images. Moreover, we found that the number of magnetic and
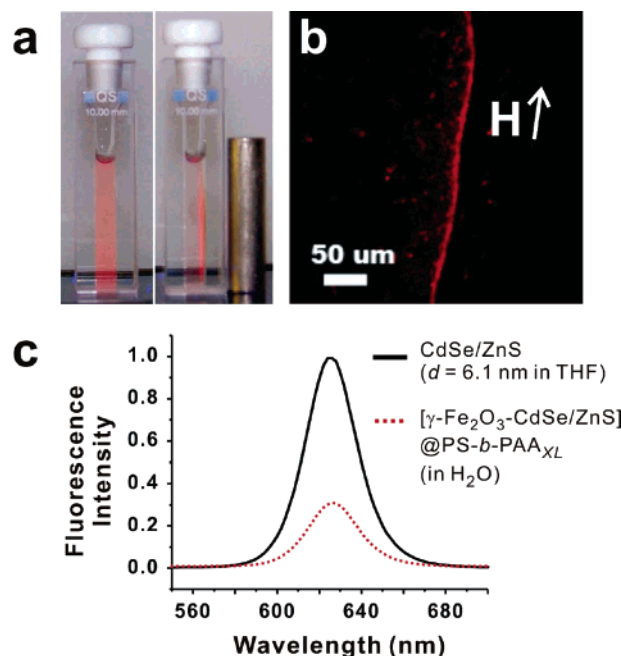
fluorescent particles in a micelle could be tuned by varying the amount of particles suspended in the initial organic solution. We observed that more particles were encapsulated as the initial concentration of nanoparticles increased. The number of particles encased in each micelle followed a roughly Gaussian distribution, which is consistent with our previous study of micelles containing only hydrophobic γ-Fe$_2$O$_3$ nanoparticles,[25] in which the nanoparticles were distributed between micelles as simple hydrophobic solubilizates.[35] As a result of this distribution, we were unable to synthesize micelles containing solely one γ-Fe$_2$O$_3$ and one CdSe/ZnS nanoparticle in this study. Instead, at limiting nanoparticle concentrations, we observed a large fraction of micelles containing only single γ-Fe$_2$O$_3$ or single CdSe/ZnS nanoparticles (Figure S2),[36] which were difficult to separate from colocalized [γ-Fe$_2$O$_3$-CdSe/ZnS]@PS-*b*-PAA$_{XL}$ micelles by centrifugation due to very low density differences between them.

As expected, the [γ-Fe$_2$O$_3$-CdSe/ZnS]@PS-*b*-PAA$_{XL}$ micelles preserved the combined properties of each component—specifically, the magnetic properties of the γ-Fe$_2$O$_3$ nanoparticles and the optical properties of the CdSe/ZnS quantum dots. The fluorescence of the QDs in the micelles was clearly visible under illumination by a handheld UV lamp, and their peak emission wavelength ($\lambda_{em,max}$ = 626 nm for $d = 6.1$ nm) and peak width (fwhm = 36 nm) were the same as before encapsulation, even after storage under room light for a month (Figure 2a,c). Likewise, the encapsulated γ-Fe$_2$O$_3$ nanoparticles made the micelles magnetic. The [γ-Fe$_2$O$_3$-CdSe/ZnS]@PS-*b*-PAA$_{XL}$ product was

(33) The CdSe/ZnS core−shell quantum dot nanoparticle was purchased from Evident Technologies and used as received.

(34) Huang, H. Y.; Remsen, E. E.; Kowalewski, T.; Wooley, K. L. *J. Am. Chem. Soc.* **1999**, *121*, 3805−3806.

(35) Zhao, J. X.; Allen, C.; Eisenberg, A. *Macromolecules* **1997**, *30*, 7143−7150.
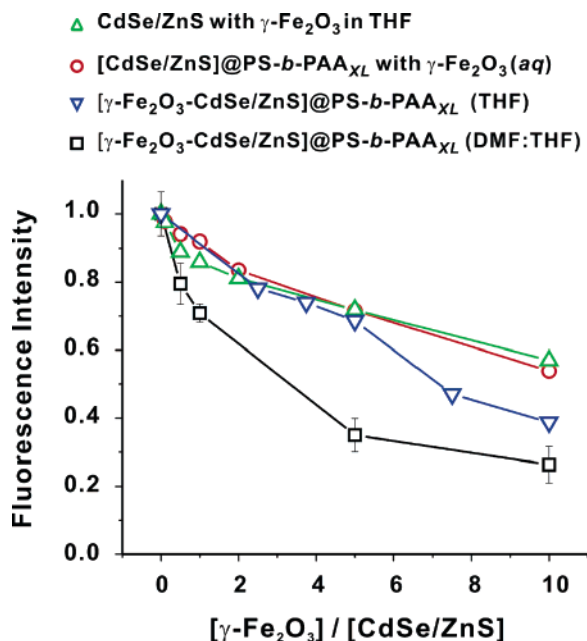
(36) See Supporting Information for details.

Figure 3. Relative fluorescence intensities of [γ-Fe$_2$O$_3$-−CdSe/ZnS]@PS-*b*-PAA$_{XL}$ micelles, as well as mixtures of γ-Fe$_2$O$_3$ and CdSe/ZnS nanoparticles, made with different ratios of γ-Fe$_2$O$_3$ to CdSe/ZnS (λ_{ex} = 400 nm): ($\triangle$) TOPO-capped CdSe/ZnS and oleic acid-capped γ-Fe$_2$O$_3$ mixed in THF; ($\bigcirc$) [CdSe/ZnS]@PS-*b*-PAA$_{XL}$ combined with TMAOH-stabilized aqueous γ-Fe$_2$O$_3$ (d = 11 nm); ($\triangledown$) [γ-Fe$_2$O$_3$-CdSe/ZnS]@PS-*b*-PAA$_{XL}$ synthesized from 100% THF; and ($\square$) [γ-Fe$_2$O$_3$-CdSe/ZnS]@PS-*b*-PAA$_{XL}$ synthesized from DMF/THF (20 vol % DMF). The concentration of CdSe/ZnS was constant (2.0 nM) in all experiments. Within each data set, the fluorescence intensity is normalized to the intensity for materials lacking γ-Fe$_2$O$_3$.

well-dispersed in the absence of magnetic field, but placing a bar magnet on the side of the container attracted all fluorescent particles to the inner container wall in a few hours (Figure 2a). This process was fully reversible; when the magnet was removed, the magnetic suspension redispersed rapidly with simple agitation without leaving any noticeable aggregates, as we previously observed for micelles containing only magnetic particles.[25] Fluorescence microscopy (Figure 2b) and TEM (Figure S3)[36] showed that [γ-Fe$_2$O$_3$-CdSe/ZnS]@PS-*b*-PAA$_{XL}$ micelles align along applied field lines, as is typically observed for magnetic nanoparticles near the paramagnetic limit.[37]

We did observe that the quantum yield (QY) of the QDs was reduced by encapsulation with magnetic γ-Fe$_2$O$_3$ nanoparticles. For [γ-Fe$_2$O$_3$-CdSe/ZnS]@PS-*b*-PAA$_{XL}$ micelles prepared in DMF/THF mixture containing 100 μg of γ-Fe$_2$O$_3$ and 2 μg of CdSe/ZnS (as in Figure 1a), for example, QY = 0.03, which is about one-fourth of that of the QDs before encapsulation (QY = 0.13), whereas the micelles prepared in the pure THF conditions exhibited a higher QY of 0.05. We also found that the QY of [γ-Fe$_2$O$_3$-CdSe/ZnS]@PS-*b*-PAA$_{XL}$ decreased further with increasing fraction of encapsulated magnetic nanoparticles (Figure 3). In principle, the fluorescence of encapsulated QDs could be reduced by physical or chemical quenching, either by the magnetic γ-Fe$_2$O$_3$ nanoparticles or by some other component of the suspension, or by simple absorption of excitation or emission light (inner filter effect). Dubertret and co-workers previously observed diminished QD fluorescence by high concentrations of α-Fe$_2$O$_3$ nanoparticles in the droplets of an oil-in-water emulsion
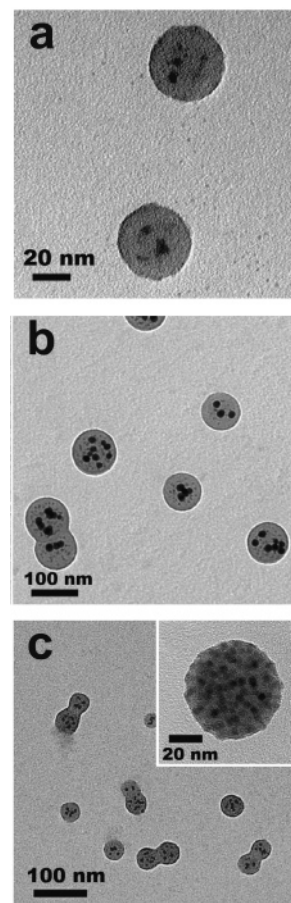

Figure 4. TEM micrographs of multicomponent hybrid micelles prepared from combinations of different nanoparticles: (a) [CdSe/ZnS-CdSe/ZnS]@PS-*b*-PAA$_{XL}$; (b) [Au-Fe$_3$O$_4$]@PS-*b*-PAA$_{XL}$; (c) [Fe$_3$O$_4$-CdSe/ZnS]@PS-*b*-PAA$_{XL}$; and (inset) densely packed [Fe$_3$O$_4$-CdSe/ZnS]@PS-*b*-PAA$_{XL}$ prepared at high particle concentration. Component particles were TOPO-stabilized CdSe/ZnS (d = 2.9 and 6.1 nm) and oleylamine-coated Fe$_3$O$_4$ (d = 4.5 nm) and Au (d = 13 nm). See Supporting Information for details.

and argued that both inner filter effects and dynamic quenching were responsible.[18] Nie and co-workers similarly attributed reduced fluorescence in QD- and Fe$_3$O$_4$-doped mesoporous silica beads to adventitious absorbance.[38] In the suspensions described here, by contrast, the contribution to optical density by the magnetic particles was negligible, ruling out inner filter effects. Presuming that dynamic quenching by γ-Fe$_2$O$_3$ would be enhanced by physical proximity to the QDs, we also measured the fluorescence of simple mixtures of QDs and γ-Fe$_2$O$_3$ nanoparticles in organic solvent, as well as mixtures of water-soluble γ-Fe$_2$O$_3$[30] and micelle encapsulated QDs[26] (Figure 3). Interestingly, the fluorescence in both of these mixtures was also reduced by increasing concentrations of γ-Fe$_2$O$_3$, regardless of solvent or of whether the QDs were encapsulated or not, even though the particle concentrations were extremely low (nM). Quenching appeared to be slightly enhanced by co-encapsulation of the two particle types in single-micelle containers. These observations indicate dynamic quenching by the magnetic nanoparticles themselves, and similar reports of dynamic quenching of fluorophores by magnetic nanoparticles have been reported.[17,18,39−41] Nevertheless, quenching by chemical contaminants, such as surface ligands and solvents, cannot be ruled out.

(37) Butter, K.; Bomans, P. H. H.; Frederik, P. M.; Vroege, G. J.; Philipse, A. P. *Nat. Mater.* **2003**, *2*, 88−91.

(38) Sathe, T. R.; Agrawal, A.; Nie, S. *Anal. Chem.* **2006**, *78*, 5627−5632.
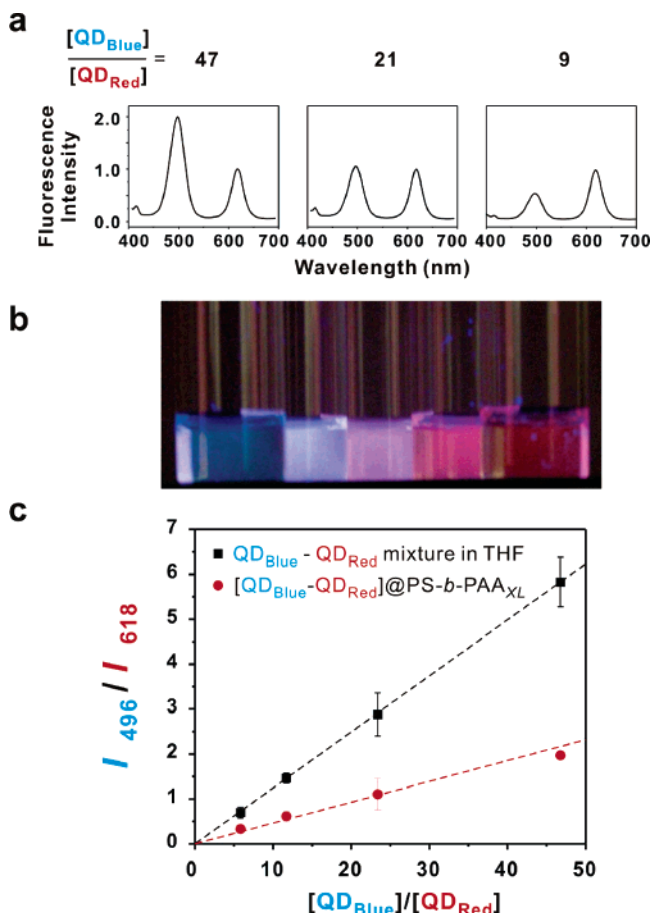
Figure 5. Multicolor [CdSe/ZnS$_{Blue}$-CdSe/ZnS$_{Red}$]@PS-*b*-PAA$_{XL}$ micelles with programmed fluorescence intensity ratios. (a) Fluorescence spectra of micelles made with different ratios of CdSe/ZnS$_{Blue}$ to CdSe/ZnS$_{Red}$, at a fixed CdSe/ZnS$_{Red}$ concentration (2.0 nM). (b) Photo of [CdSe/ZnS$_{Blue}$-CdSe/ZnS$_{Red}$]@PS-*b*-PAA$_{XL}$ micelles made to have (from left to right) 2:0, 2:1, 1:1, 1:2, and 0:2 relative fluorescence intensity ratio of CdSe/ZnS$_{Blue}$ to CdSe/ZnS$_{Red}$. (c) Ratio of fluorescence intensity at $\lambda = 496$ nm to $\lambda = 618$ nm for mixtures of CdSe/ZnS$_{Blue}$ and CdSe/ZnS$_{Red}$: (■) mixture of TOPO-capped CdSe/ZnS nanoparticles in THF and (●) [CdSe/ZnS$_{Blue}$-CdSe/ZnS$_{Red}$]@PS-*b*-PAA$_{XL}$ micelles. The concentration of CdSe/ZnS$_{Red}$ was held constant (2.0 nM).

Because assembly of these nanoparticles depends only on simultaneous desolvation of nanoparticles and amphiphilic block copolymers, and not on any specific polymer−surface interaction, we were able to extend this approach to other combinations of nanoparticles, including CdSe/ZnS of different sizes, Au, and Fe$_3$O$_4$ (Figure 4). In all cases, the properties of both nanoparticle

components were successfully integrated into the compound nanostructure. For example, [CdSe/ZnS$_{Blue}$-CdSe/ZnS$_{Red}$]@PS-*b*-PAA$_{XL}$ (QD$_{Blue}$ − QD$_{Red}$) micelles containing two different diameters of CdSe/ZnS nanoparticles ($d = 2.9$ and 6.1 nm)[33] fluoresced at both emission wavelengths of the component QDs (Figure 5). In addition, by combining different amounts of each QD in the initial polymer−particle solution, we were able to precisely control the intensity of each fluorescence emission of the multicolor QD$_{Blue}$ − QD$_{Red}$ micelles without spectral overlap or wavelength shifting (Figure 5a). In principle, the distinct multiple fluorescence profiles of these compound particles would make them useful in fluorescence intensity multiplexing,[42] where the relative intensities of the two fluorophores would be indexed to a particular analyte or target.

Because of the differences in extinction coefficients and quantum yields between the two QDs, the ratio of CdSe/ZnS$_{Blue}$ to CdSe/ZnS$_{Red}$ particles required to produce a 1:1 ratio of blue to red fluorescence was much greater than 1 (Figure 5). Nevertheless, encapsulated mixtures of blue and red CdSe/ZnS nanoparticles exhibited predictable fluorescence intensities at the two emission wavelengths. Unlike γ-Fe$_2$O$_3$, neither of the QDs appeared to significantly affect the fluorescence intensity of the other, and the contribution to overall fluorescence was linear with QD concentration for both QDs (Figure 5c). We did not expect to observe fluorescence resonance energy transfer (FRET) from CdSe/ZnS$_{Blue}$ to CdSe/ZnS$_{Red}$ in this system, both because very few CdSe/ZnS$_{Blue}$ particles should have CdSe/ZnS$_{Red}$ neighbors at the particle ratios used here and because the absorbance of CdSe/ZnS$_{Blue}$ is much less than that of CdSe/ZnS$_{Red}$ at all excitation wavelengths with a given concentration.

Conclusion

In conclusion, we have demonstrated that multifunctional nanostructures can be synthesized by encapsulating different component nanoparticles within cross-linked, block copolymer micelles. The method is simple and can be used with any combination of hydrophobic nanoparticles to incorporate multiple desirable properties in a single, water-soluble nanoscale container. Block copolymer micelles have been used in a wide variety of biomedical applications in vivo, and we anticipate that multi-component micelle encapsulated particles could be similarly useful as targeted drug delivery agents, long-circulating scaffolds for biomolecule presentation, and tags for tracking cells. As we have demonstrated previously for other micelle encapsulated nanostructures,[25] the presence of functional groups on the polymer shell should permit further functionalization on the outer surface of the hybrid micelles, which will broaden their potential applications in biotechnology.

Supporting Information Available: Detailed procedures for the preparation of other hybrid micelles and additional TEM images. This material is available free of charge via the Internet at http://pubs.acs.org.

(42) Bradford, J. A.; Buller, G.; Suter, M.; Ignatius, M.; Beechem, J. M. *Cytometry* **2004**, *61A*, 142−152.
(43) Turro, N. J.; Lakshminarasimhan, P. H.; Jockusch, S.; O'Brien, S. P.; Grancharov, S. G.; Redl, F. X. *Nano Lett.* **2002**, *2*, 325−328.
(44) Cherepy, N. J.; Liston, D. B.; Lovejoy, J. A.; Deng, H. M.; Zhang, J. Z. *J. Phys. Chem. B* **1998**, *102*, 770−776.
(45) Oliveira, D. M.; Macaroff, P. P.; Ribeiro, K. F.; Lacava, Z. G. M.; Azevedo, R. B.; Lima, E. C. D.; Morais, P. C.; Tedesco, A. C. *J. Magn. Magn. Mater.* **2005**, *289*, 476−479.